

# Hole-doped manganites based tunneling junctions with isostructural barrier layer

Y. LIU<sup>a, b, \*</sup>, Z. LI<sup>a</sup>, Y. WANG<sup>b</sup>, H. YAN<sup>c</sup>

<sup>a</sup>College of Physics and Electronic Engineering, Taizhou University, Taizhou, Zhejiang 318000, China

<sup>b</sup>Department of Physics, Lanzhou University, Lanzhou, Gansu 730000, China

<sup>c</sup>Laboratory of Thin Film Materials, Beijing University of Technology, Beijing, Beijing 100022, China

La<sub>0.7</sub>Sr<sub>0.3</sub>MnO<sub>3</sub>/La<sub>0.96</sub>Sr<sub>0.04</sub>MnO<sub>3</sub>/La<sub>0.7</sub>Sr<sub>0.3</sub>MnO<sub>3</sub> magnetic tunnel junction device have been fabricated on SrTiO<sub>3</sub> (STO) substrate. A large tunneling magnetoresistance (TMR) of 134% was observed from the junction with an antiferromagnetic insulating barrier layer (2 nm) at a temperature 4.2 K. Current-voltage (I-V) characteristic of the junction is consistent with a tunneling process at low temperature. A simulation based on Simmons' tunneling model give a barrier-layer thickness  $d \approx 5$  nm and an average barrier potential height  $\Phi \approx 0.1$  eV, respectively. The results indicate that the large TMR is related to crystallographic similarity between La<sub>0.7</sub>Sr<sub>0.3</sub>MnO<sub>3</sub> and La<sub>0.96</sub>Sr<sub>0.04</sub>MnO<sub>3</sub> compounds, which should minimize lattice mismatch between the electrodes and the barrier layers.

(Received July 30, 2010; accepted August 12, 2010)

**Keywords:** Magnetic tunnel junction, Tunneling magnetoresistance, Spin polarization, Manganite

## 1. Introduction

Spin-based magnetic tunnel junctions (MTJ) incorporated with ferromagnetic (FM) electrode layers and an insulator layer show a high tunneling magnetoresistance (TMR) because of the difference in resistance between the parallel and antiparallel magnetization configurations of the FM layers. The TMR effect has been observed in devices with electrodes of colossal magnetoresistance (CMR) materials as well as ferromagnetic metals. Half-metallic ferromagnets were predicated to be able to produce a high magnetic-field sensitivity for nearly 100% spin polarization of conduction carriers [1-3]. In technology, CMR materials, such as La<sub>1-x</sub>A<sub>x</sub>O<sub>3</sub> (where A stands for alkaline earth element), have been extensively studied by various methods, including spin-polarized photoemission [2], and spin-polarized tunnel junction [4-6]. Studies have shown that CMR-based junctions can exhibit TMR even at a temperature as high as 295 K [7, 8].

In CMR-based magnetic tunnel junctions, the material of tunnel barrier has primarily been a nonmagnetic insulator SrTiO<sub>3</sub> (STO) [9]. However, the lattice mismatch (1.6%) between STO and La<sub>0.7</sub>Sr<sub>0.3</sub>MnO<sub>3</sub> may result in unwanted effects on interface quality and observed TMR. Obata et al. obtained a small junction magnetoresistance for a La<sub>0.7</sub>Sr<sub>0.3</sub>MnO<sub>3</sub>/SrTiO<sub>3</sub>/La<sub>0.7</sub>Sr<sub>0.3</sub>MnO<sub>3</sub> junction with a 1.6 nm barrier layer at 5K [7]. To minimize lattice mismatch between the electrodes and barrier, Yin et al. have incorporated an isostructural manganite tunnel barrier of La<sub>0.85</sub>Sr<sub>0.15</sub>MnO<sub>3</sub> and obtained magnetoresistance of 4%-6% at temperature close to room temperature [5]. Alldredge et al. used La<sub>0.35</sub>Ca<sub>0.65</sub>MnO<sub>3</sub> barrier with

La<sub>0.7</sub>Sr<sub>0.3</sub>MnO<sub>3</sub> electrodes and obtained a large junction magnetoresistances of 4% at 5 K [10]. Therefore, in a tri-layer TMR device, a perfectly epitaxial magnetic-nonmagnetic interface with very few defects would probably be a good solution for increasing the value of TMR.

In this study, a TMR device with tri-layer configuration La<sub>0.7</sub>Sr<sub>0.3</sub>MnO<sub>3</sub>/La<sub>0.96</sub>Sr<sub>0.04</sub>MnO<sub>3</sub>/La<sub>0.7</sub>Sr<sub>0.3</sub>MnO<sub>3</sub> MTJ was fabricated on STO substrate. According to the phase diagram of La<sub>1-x</sub>Sr<sub>x</sub>MnO<sub>3</sub>, La<sub>0.96</sub>Sr<sub>0.04</sub>MnO<sub>3</sub> and La<sub>0.7</sub>Sr<sub>0.3</sub>MnO<sub>3</sub> are antiferromagnetic insulator and metal ferromagnetic below room temperature, respectively. Although an antiferromagnetic has magnetic spins, the high-energy cost to flip a spin, due to the long range magnetic order, may preserve spin orientation during transport. A large TMR value of 134% was obtained in this device. The crystallographic similarity between La<sub>0.7</sub>Sr<sub>0.3</sub>MnO<sub>3</sub> and La<sub>0.96</sub>Sr<sub>0.04</sub>MnO<sub>3</sub> compounds was believed to minimize lattice mismatch between the electrodes and barrier, which could eliminate the interface states that degraded the TMR performance.

## 2. Experimental

La<sub>0.7</sub>Sr<sub>0.3</sub>MnO<sub>3</sub>(100nm)/La<sub>0.96</sub>Sr<sub>0.04</sub>MnO<sub>3</sub>(2nm)/La<sub>0.7</sub>Sr<sub>0.3</sub>MnO<sub>3</sub>(100 nm) tri-layer structures were deposited on (100) oriented 10×10 mm<sup>2</sup> STO substrate by radio frequency magnetron sputtering. The films deposition was carried out in argon balanced with 20 vol% oxygen and the total pressure during sputtering was 1 Pa. The substrate temperature was controlled at 700-750 °C. After each layer deposited, the sample was *in situ* annealed in oxygen

atmosphere at deposited temperature to passivate surface of the film, improve the film quality and increase the oxygen content in the film. A platinum layer of 20 nm was deposited *ex situ* by dc magnetron sputtering on the trilayer to protect the top electrode from possible damage. A patterning process was carried out by UV photolithography techniques and Ar ion etching. The junction of elliptical shape with long axis of 12 $\mu$ m and short axis of 6  $\mu$ m was obtained.

### 3. Results and discussion

Fig. 1 shows XRD pattern of a TMR device with tri-layer configuration  $\text{La}_{0.7}\text{Sr}_{0.3}\text{MnO}_3$  (100 nm)/ $\text{La}_{0.96}\text{Sr}_{0.04}\text{MnO}_3$  (2 nm)/ $\text{La}_{0.7}\text{Sr}_{0.3}\text{MnO}_3$  (100 nm) on (100) STO substrate. The result indicates that the tri-layer films are (100) oriented in the growth direction, which is in accordance with the orientation of the (100) STO substrate.

Transport measurements were performed by a four-probe measurement and Physical Property Measurement System (PPMS). Fig. 2 describes the planar view of a MTJ using a  $\text{La}_{0.7}\text{Sr}_{0.3}\text{MnO}_3/\text{La}_{0.96}\text{Sr}_{0.04}\text{MnO}_3/\text{La}_{0.7}\text{Sr}_{0.3}\text{MnO}_3$  tri-layer. A voltage,  $V_{\text{DC}}$ , applied on TMR device was 10 mV. The direction of magnetic field was along the longitudinal of top LSMO electrode. In general, LSMO film deposited on STO substrate, the films are under tensile strain due to the lattice mismatch between the films and substrate. Therefore, the bottom electrode and top electrode show different coercive field due to different strain situation of two electrodes. When the magnetic field switches from high field to low field, the bottom electrode flips first, and then the top electrode flips more gradually at a higher field.

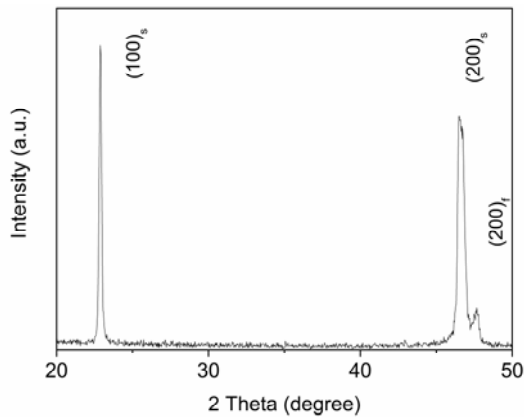


Fig.1. XRD pattern of a TMR device with the tri-layer configuration  $\text{La}_{0.7}\text{Sr}_{0.3}\text{MnO}_3/\text{La}_{0.96}\text{Sr}_{0.04}\text{MnO}_3/\text{La}_{0.7}\text{Sr}_{0.3}\text{MnO}_3$ .

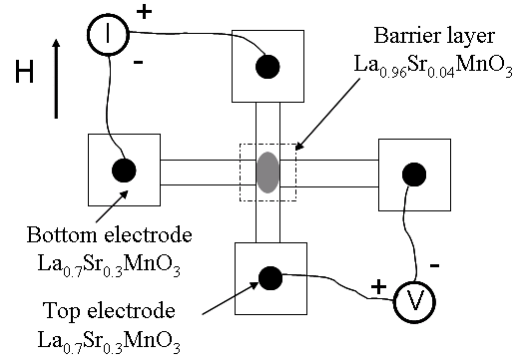


Fig. 2. A planar view of a MTJ using a  $\text{La}_{0.7}\text{Sr}_{0.3}\text{MnO}_3/\text{La}_{0.96}\text{Sr}_{0.04}\text{MnO}_3/\text{La}_{0.7}\text{Sr}_{0.3}\text{MnO}_3$  tri-layer structure.

The magnetic field dependence of resistance and TMR ratio for a tri-layer TMR device at 4.2 K is shown in Fig. 3. The magnetic moments of top and bottom  $\text{La}_{0.7}\text{Sr}_{0.3}\text{MnO}_3$  electrodes are aligned in parallel for high magnetic fields, while they are anti-parallel in low fields due to the difference in the coercivities. Thus, TMR is high in the antiparallel configuration of the magnetic moments in low fields, and low in the parallel configuration in high fields. The peak of TMR in the switching field, where the magnetic moments of the LSMO electrodes are realigned from parallel to antiparallel, suggests an entire flip of the magnetic domains against a magnetic field. While the resistance of top and bottom electrodes is much smaller than the junction resistance, the junction resistance is believed to be dominated by the insulating barrier and, also probably, by the interface states between electrodes and barrier. As seen in Fig. 3, the junction resistance varies from  $1.1 \times 10^6 \Omega$  (antiparallel) to  $4.7 \times 10^5 \Omega$  (parallel) with the change of applied magnetic field. TMR ratio is defined as [11]:

$$TMR = (R_{AP} - R_p) / R_p = 2P_1P_2 / (1 - P_1P_2) \quad (1)$$

where  $R_{AP}$  and  $R_p$  are the resistance of the junction in the antiparallel and parallel configurations, respectively.  $P_1$  and  $P_2$  are spin polarizations of the two ferromagnetic electrodes. As the top and bottom electrodes were fabricated under the same condition, the polarization of both electrodes were considered to be equal ( $P_1=P_2=P$ ) [12]. TMR ratio determined from Eq. (1) is 134% from the difference between the parallel and antiparallel magnetization configurations of the FM layers. The spin polarization of FM electrodes is approximately 63.3%,

which is larger than that in typical ferromagnetic metals (20%-50%) [12, 13]. Compared with the ideal value of spin polarization of FM electrodes (100%), the smaller experimental value may be due to existence of a low-height barrier region, as discussed in next section. The barrier region is believed to locate between the electrodes and barrier layer, which degraded the polarization performance.

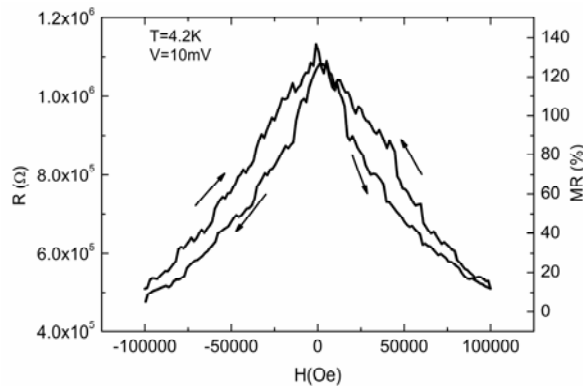


Fig. 3. Magnetic field dependence of the junction resistance and tunneling magnetoresistance ratio for a tri-layer TMR device at 4.2 K.

To clarify the mechanism of magnetoresistance, we further measured the current-voltage (I-V) characteristic of the tri-layer TMR device. The non-linear current-voltage characteristic at temperature of 4.2 K indicates that there is a non-ohmic conduction in TMR device, as seen in Fig. 4. Fig. 5 shows the direct current conductance  $G=dI/dV$  normalized by the conductance  $G_0$  at zero voltage as a function of junction bias. The parabolic shape of  $G/G_0$  versus  $V$  curve shows that a tunneling process controls the conduction. By fitting the raw data of I-V characteristic to the Simmons equation [14], we obtained a barrier thickness of about 5 nm and an average barrier height  $\Phi \approx 0.1$  eV. The barrier thickness is larger than the designed thickness (2 nm). Yin et al. proposed that a low barrier potential height was expected from lower resistivity of the barrier layer [15]. In our case, as shown in Fig. 3, the resistance varied from  $10^5$  to  $10^6 \Omega$ . A possible explanation for this result is that part of the  $\text{La}_{0.7}\text{Sr}_{0.3}\text{MnO}_3$  layer adjacent to the  $\text{La}_{0.7}\text{Sr}_{0.3}\text{MnO}_3/\text{La}_{0.96}\text{Sr}_{0.04}\text{MnO}_3$  interface acts as a low height barrier region, which increases the barrier thickness and decreases the average barrier height and thus degrades the spin polarization of FM electrodes. We believe that the formation of a low height barrier region is due to the uncontrollable factors during the fabricating process. In addition, the low height barrier region could impede the flip of the magnetic moments at the barrier interface, similar results also reported in ref. 10, which is very disadvantaged for TMR application.

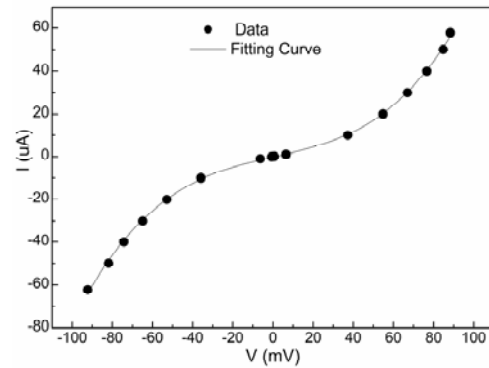


Fig. 4. Current-voltage characteristic of tri-layer TMR device at low temperature of 4.2 K.

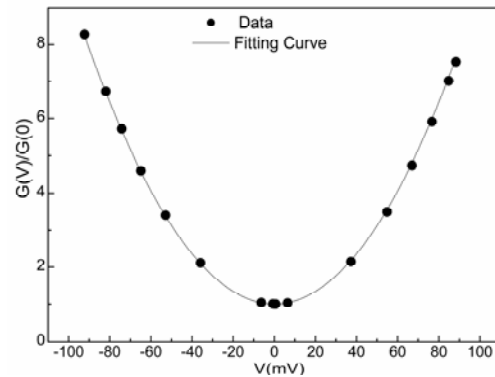


Fig. 5. Direct current conductance  $G=dI/dV$  normalized by the conductance  $G_0$  at zero voltage as a function of junction bias.

Although the low-height barrier region existed in the device, the large TMR of 134% was obtained. The crystallographic similarity between  $\text{La}_{0.7}\text{Sr}_{0.3}\text{MnO}_3$  and  $\text{La}_{0.96}\text{Sr}_{0.04}\text{MnO}_3$  compounds is expected to minimize the lattice mismatch. To further confirm the argument, a  $\text{La}_{0.7}\text{Sr}_{0.3}\text{MnO}_3(100 \text{ nm})/\text{STO}(2 \text{ nm})/\text{La}_{0.7}\text{Sr}_{0.3}\text{MnO}_3(100 \text{ nm})$  tri-layer MTJ have also been fabricated under the same conditions. The TMR value is much smaller than the reported device. Therefore, the selection of barrier layer of MTJ is essential for improving its magnetotransport properties.

For a  $\text{La}_{0.7}\text{Sr}_{0.3}\text{MnO}_3/\text{La}_{0.96}\text{Sr}_{0.04}\text{MnO}_3/\text{La}_{0.7}\text{Sr}_{0.3}\text{MnO}_3$  junction, it is expected that a higher TMR can be obtained by optimized design and using advanced device technology.

#### 4. Conclusions

$\text{La}_{0.7}\text{Sr}_{0.3}\text{MnO}_3/\text{La}_{0.96}\text{Sr}_{0.04}\text{MnO}_3/\text{La}_{0.7}\text{Sr}_{0.3}\text{MnO}_3$  magnetic tunnel junction was fabricated on STO substrate. A large TMR effect was observed at low temperature of 4.2 K, which was dominated by the crystallographic similarity between the electrodes and barrier layer. According to the Simmons' tunneling model, we believe that a low height barrier region formed in the MTJ device. The results indicate that the antiferromagnetic insulator  $\text{La}_{0.96}\text{Sr}_{0.04}\text{MnO}_3$  might be a promising candidate for the

barrier layer of LSMO based MTJ to improve its magnetotransport properties.

### References

- [1] Y. Okimoto, T. Katsufuji, T. Ishikawa, A. Urushibara, T. Arima, Y. Tokura, *Phys. Rev. Lett.* **75**, 109 (1995).
- [2] J. H. Park, E. Vescovo, H. J. Kim, C. Kwon, R. Ramesh, T. Venkatesan, *Nature* **392**, 794 (1998).
- [3] W. E. Pickett, D. J. Singh, *Phys. Rev. B* **53**, 1146 (1996).
- [4] J. Z. Sun, D. W. Abraham, K. Roche, S. S. P. Parkin, *Appl. Phys. Lett.* **73**, 1008 (1998).
- [5] H. Q. Yin, J. S. Zhou, J. B. Goodenough, *Appl. Phys. Lett.* **77**, 714 (2000).
- [6] D. Ozkaya, A. K. Petford-Long, M. H. Jo, M. G. Blamire, *J. Appl. Phys.* **89**, 6757 (2001).
- [7] T. Obata, T. Manako, Y. Shimakawa, Y. Kubo, *Appl. Phys. Lett.* **74**, 290 (1999).
- [8] M. H. Jo, N. D. Mathur, N. K. Todd, M. G. Blamire, *Phys. Rev. B* **61**, R14905 (2000).
- [9] M. Viret, M. Drouet, J. Nassar, J. P. Contour, C. Fermon, A. Fert, *Europhys. Lett.* **39**, 545 (1997).
- [10] L. M. B. Aldredge, Y. Suzuki, *Appl. Phys. Lett.* **85**, 437 (2004).
- [11] M. Julliere, *Phys. Lett.* **54A**, 225 (1975).
- [12] X. F. Han, M. Oogane, H. Kubota, Y. Ando, T. Miyazaki, *Appl. Phys. Lett.* **77**, 283 (2000).
- [13] P. M. Tedrow, R. Meservey, *Phys. Rev. B* **7**, 318 (1973).
- [14] J. G. Simmons, *J. Appl. Phys.* **35**, 2655 (1964).
- [15] H. Q. Yin, J. S. Zhou, K. Sugawara, J. B. Goodenough, *J. Magn. Magn. Mater.* **222**, 115 (2000).

---

\*Corresponding author: yepylus@163.com